Kinetics and Thermodynamics of Uranium Adsorption Using Impregnated Magnetic Graphene Oxide

Gado, Mohamed A.; Atia, Bahig M.; Hagag, Mohamed. S.
Nuclear Materials Authority, 530 P.O Box Maadi, Cairo, EGYPT

ABSTRACT: *Magnetic Graphene Oxide (MGO) impregnated Di(2-Ethyl Hexyl)Phosphoric Acid (D2EHPA) (DMGO) was prepared by multi-impregnation. The structures of GO and DMGO were characterized by FT-IR, TGA, EDX, SEM, and XRD. The adsorption capacities for U(VI) from aqueous solution is 154.4 mg/g at pH 5. The essential factors that affected U(VI) adsorption such as initial pH, contact time, and temperature were investigated. The adsorption is highly dependent on the solution pH. In addition, the adsorption isotherm and thermodynamics were investigated. The adsorptions of U(VI) from aqueous solution on DMGO was fitted to the Langmuir adsorption isotherms. The adsorption of U(VI) on DMGO is remarkably improved by GO impregnated with D2EHPA. Thermodynamic parameters further show that the sorption is an endothermic and spontaneous process. DMGO is a powerful promising sorbent for the efficient removal of U(VI) from aqueous solutions.*

KEYWORDS: *Uranium. Adsorption; D2EHPA; Graphene oxide; Impregnation.*

INTRODUCTION

Uranium is a radioactive metal that occurs in nature and plays an important role in the nuclear industry. It is usually a product of uranium mining and hydrometallurgy. Unfortunately, a large amount of low concentration uranium-containing radioactive wastewater is produced at the same time. Uranium contamination, even at trace levels, is a threat to human health and the environment because of its chemical toxicity and radioactivity [1-3].

Many approaches, including adsorption [4-7], bioreduction, precipitation [8, 9], electrodialysis, reverse osmosis [10], ion exchange [11, 12], and membrane filtration, have been applied to eliminate U(VI) from wastewater. Among these methods, adsorption technology has its unique merits for practical and large-scale applications, such as easy operation, high efficiency, etc [4], as well as several drawbacks, including limited adsorption capacity, restricted adsorption conditions, especially for solution pH value. Therefore, new adsorbents with high adsorption capacity and mild adsorption conditions are still required for radionuclides treatment.

Different types of adsorbents have been developed for uranium (VI) removal in an economical manner, such as inorganic oxides [13], metal-organic frameworks [14], and biomass [15]. However, most of these materials have no resistance to the acidic environment, and to radiation [16**]**.

For these reasons, carbon materials are promising candidates for use because of their thermal and radiation stabilities. Graphene, a monolayer of graphite,

** To whom correspondence should be addressed.*
+ E-mail: parq28@yahoo.com
1021-9986/2020/5/225-237 13/$/6.03

with its advantageous thermal and mechanical properties, has been used in many areas, such as electrochemical energy storage, solar cells and gas adsorption [17, 18].

Carbonaceous materials including Activated Carbon (AC), biochar, Carbon NanoTubes (CNTs), and Graphene Oxide (GO) have been widely studied for adsorption of various environmental contaminants [19-21] Graphene Oxide (GO) is the oxidized form of graphene and is decorated with epoxy, hydroxyl, keto, and carboxyl reactive oxygen functional groups.

Graphene Oxide (GO) is typically obtained by oxidation or sonication of graphite, its also the oxidized form of graphene which possesses oxygen-containing functional groups, including hydroxyl groups (–OH), epoxy groups (–C=O), and carboxyl groups (–COOH). In addition, GO also possesses a high specific surface area [22]

Compared to other carbon-based materials, GO exhibits better environmental compatibility and biocompatibility. Oxygen-containing functional groups can be used as the adsorption sites for heavy metal ions in wastewater [23]. Through interaction with these oxygen-containing functional groups, heavy metal ions can be removed from wastewater, thus enabling purification [24]. In addition, the presence of these functional groups enables the stable dispersion of GO in water and other polar organic solvents [25].

The GO adsorption affinity to many metal ions is sturdy, and varies from the types of metal ions. The higher electronegativity of metal ions, the stronger attraction of the metal ions on the negatively charged GO surface. In addition, the complexation of heavy metal species with surface oxygenous functional groups (e.g. hydroxyl and carboxylic groups) was also one possible adsorption mode, and the speciation of heavy metal ion species was determined by the stability constants. The mechanisms for the adsorption of metal ions on the surface of GO were ascribed to electrostatic attraction [26], ion exchange [27] and surface complexation [28].

Graphene oxide (GO) has become a hot topic for the uptake of inorganic and organic pollutants because of its ultrahigh surface area and large mechanical strength. In particular, abundant functional groups present on the surface, and these provide a larger space for further modification [29]. The maximum adsorption capacity of graphene oxide (GO) for uranium (VI) is only 97.5 mg/g [30].

It has been proposed that introducing suitable functional groups on the surface of GO can greatly increase its adsorption capability and improve its water dispersion property, and these are important for practical applications of GO as an adsorbent. To date, researchers have prepared GO composite materials with organic functional groups, such as amidoxime, amino, imide, sulfonate, or phosphonate groups, to enhance the adsorption of U(VI) ions **[31]**.

In this study, magnetic graphene oxide was prepared and Impregnated in Di(2-Ethyl Hexyl)Phosphoric Acid (D2EHPA) in order to obtain (D2EHPA) impregnated magnetic graphene oxide (DMGO) adsorbent. The combination between D2EHPA and GO in order to increase the adsorption capacity of DMGO toward uranyl ions. DMGO characterized by Fourier Transform InfraRed (FT-IR) spectra, ThermoGravimetric Analysis (TGA), Energy-dispersive X-ray spectroscopy EDX, and Scanning Electron Microscopy (SEM). The prepared adsorbent tested for U (VI) ions removal from liquid waste solution through batch adsorption experiments.

EXPERIMENTAL SECTION

Chemicals and reagents

The starting material, is Nature large-flake graphite (325 mesh, 99.8 %) obtained from (325 mesh, 99.8%, Alfa Aesar), A stock solution of 1000 mg L^{-1} U(VI) was prepared using $UO_2(NO_3)_2.6H_2O$ which obtained from Merck Co. The stock solution of U(VI) was prepared by dissolving appropriate amounts of $UO_2(NO_3)_2.6H_2O$ in nitric acid solution for inhibition of the hydrolysis of U(VI). D2EHPA was obtained from Merck also. While all other chemicals were of analytical grade and used without further purification. All testing solutions were prepared with de-ionized water.

Spectrophotometric determination of uranium and the FT-IR spectra of the adsorbent were recorded using Jasco model V 650 and 4200 instruments respectively. An Li 127 (Elico, India) model pH meter was used for pH measurements. And The SEM images and the EDAX spectra were obtained using a JEOL JSM-6390 analyzer.

Preparation of GO nanosheets

GO was synthesized using modified hummers method as [32, 33] described in our previous work. In brief; 1 g graphite powder was added to a mixture of 3 g $NaNO_3$

and 70 mL of concentrated H_2SO_4 in an ice bath. Then, 3 g $KMnO_4$ was gradually added at 15 min under stirring. The mixture was stirred for 2 h at ambient temperature and then diluted with deionized (DI) water and stirred for 30 min. After that, 5% $H_2O_2$was added into the solution until the color of the mixture changed to yellow, indicating that graphite is fully oxidized. The as-obtained graphite oxide slurry was re-dispersed in DI water and then exfoliated to generate graphene oxide nanosheets using a bath ultrasonic. The mixture was then, filtered and washed with diluted HCl solution to remove metal ions. Finally, the product was washed with DI water to remove the acid.

Preparation of magnetic graphene oxide MGO

The magnetic graphene oxide has been prepared using the modified method of Massart [34], where about 100 mL from ferric solution (0.2 M) has been mixed with 100 mL from freshly prepared 0.1 M ferrous solution under stirring with ten gram from the produced porous carbon. After that, about 100 ml from ammonia solution (30 %) has been poured to the Fe^{+3}/Fe^{+2}/GO mixture and stirred vigorously. A black precipitate has been formed which was left to crystallize for 30 min. under stirring. The crystallized product has been then washed with deoxygenated water under magnetic decantation until pH of suspension became below 7.5. The precipitate was dried at room temperature to give a black powder and marked as MGO.

Preparation of Impregnated magnetic graphene oxide with D2EPAH (DMGO)

1.5 g of MGO was mixed with D2EHPA solution in Benzene a 100 mL reaction flask. The mixture was refluxed at 120 °C for 10 h. The reaction mixture was poured into cold water and the solid was filtered and washed with methanol, the functionalized adsorbents were finally dried at 70 °C for 7 hours to be ready for use. The DMGO were characterized by using SEM, FT-IR, EDX.

Batch adsorption experiments

Adsorption experiments under controlled pH were carried out by adding portions of 0.1 g DMGO in a series of flasks, each one containing 20 mL solution of (250 ppm) U(VI) ions solution. The pH was adapted in the range of 1–6 using nitric acid or sodium hydroxide solutions. The flasks were shaken on a shaking water bath model 1083 (Labortechnik GmbH, Germany) at 300 rpm for 2 h at 25 °C. After equilibration, the residual concentration of the metal ion was determined.

To conduct the time effect, 0.1 g of DMGO was put in a series of flasks containing 20 mL of U(VI) ions solution (250 ppm) at pH 5. The flasks were shaken on a shaking water bath for the required time period. The effect of initial concentration of U(VI) ion was carried out at definite concentrations (250–1000 ppm) and pH 5. The contents of the flasks were equilibrated on a shaking water bath while keeping the temperature at 25, 50, and 70˚C. After adsorption, the residual U(VI) concentration of the metal ion was determined. The effect of the solid/liquid ratio on the adsorption efficiency of the studied resins was achieved by varying the amount of beads from 0.01 to 0.3 g in the adsorption medium (20 mL containing 250 ppm U(VI)), while keeping other parameters (pH, contact time, and temperature) constant according to their values obtained from the previous experiments.

RESULTS AND DISCUSSIONS

Characterization of the Adsorbent

Fourier transform infrared FTIR spectra of the prepared GO and DMGO:

FT-IR was employed to evaluate the structural characteristics, the FTIR spectra of pristine GO and DMGO are presented in Fig. 1. In the spectrum of GO, there are several typical absorption peaks: the peak at 1072 cm^{-1} are related to C-O, while the peak at 1730 cm^{-1} is attributed to C=O stretching vibrations, the peak at 3430 cm^{-1} are assigned to O-H stretching, the C=C peak appears at 1620 cm^{-1} [35]. After the impregnation with D2EPAH with the surface of GO, several new peaks are observed in the spectrum of DMGO. The absorption peaks at around 600, 960 and 1020 cm^{-1} were assigned as phosphate group in-side-plane deformation vibration, symmetric bridge vibrations [36, 37], and asymmetric bridge vibrations, respectively. The bands at 1256, 1640, 1721 and 3420 cm^{-1} corresponded to the P=O absorption, P-O bond, C=O and O-H functional groups.

Thermogravimetric analysis of GO and DMGO

Thermal properties of GO and DMGO in a nitrogen atmosphere were investigated by TGA, and the results are displayed in Fig. 2. the initial mass loss of GO below 100 °C is attributed to the evaporation of the adsorbed water, and the maximum mass loss temperature (T_{max}) occurs

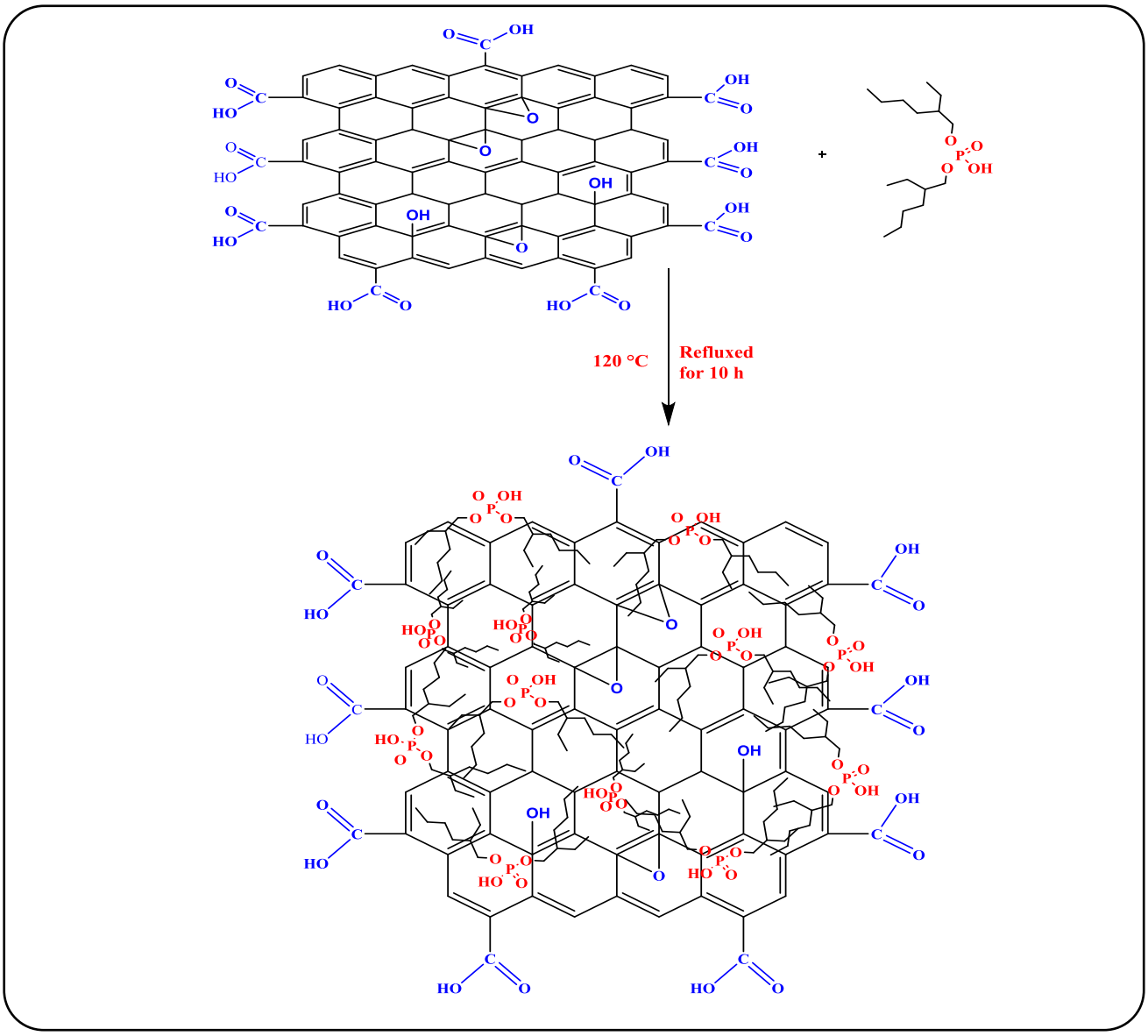

Scheme 1: Interaction of D2EHPA Impregnated magnetic graphene oxide.

at around 200 °C, due to the decomposition of labile oxygen functional groups, such as hydroxyl and carboxyl groups. The steady weight loss occurs in the temperature range of 300.700 °C, due to the degradation of the residual char, and a char yield of 53% is obtained at 700 °C. For DMGO shows two-step weight loss. The first stage is attributed to the degradation of oxygen functional groups on the surface of DMGO and the grafted flame retardant. While the second mass loss between 450 and 550 °C is assigned to the further decomposition of the residual char.

SEM and EDX pattern of MGO and DMGO

In order to identify and visualize the adsorption of U(VI) on DMGO, SEM-EDX was employed. The surface morphologies of GO and DMGO were examined with SEM, as depicted in Fig. 3. GO demonstrated a two-dimensional multilayered structure with lateral sizes of several nanometers, as the reported literature [38]. While in the DMGO, the combination with Fe_3O_4 with impregnation caused disorderness in the basal plane. Fig. 4 shows the typical EDX pattern of nanoparticle DMGO before and after uranium adsorption which indicate

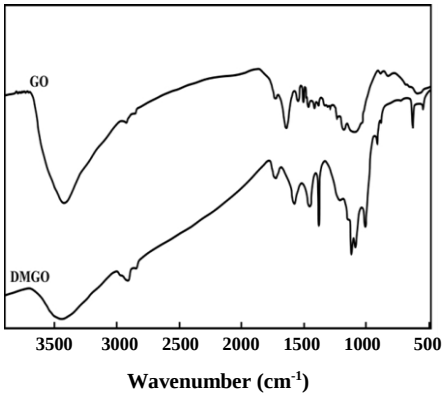

Fig. 1: The FT-IR spectra of DMGO and GO.

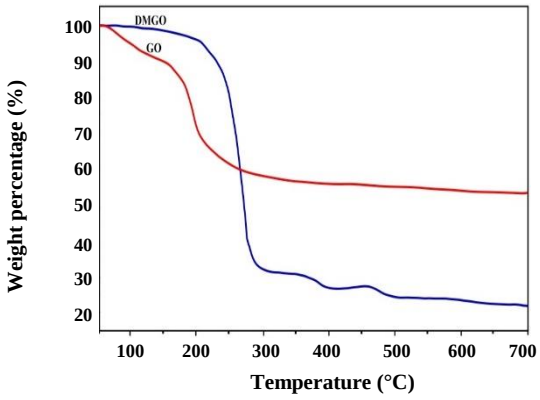

Fig. 2: Thermogravimetric analysis of GO and DMGO.

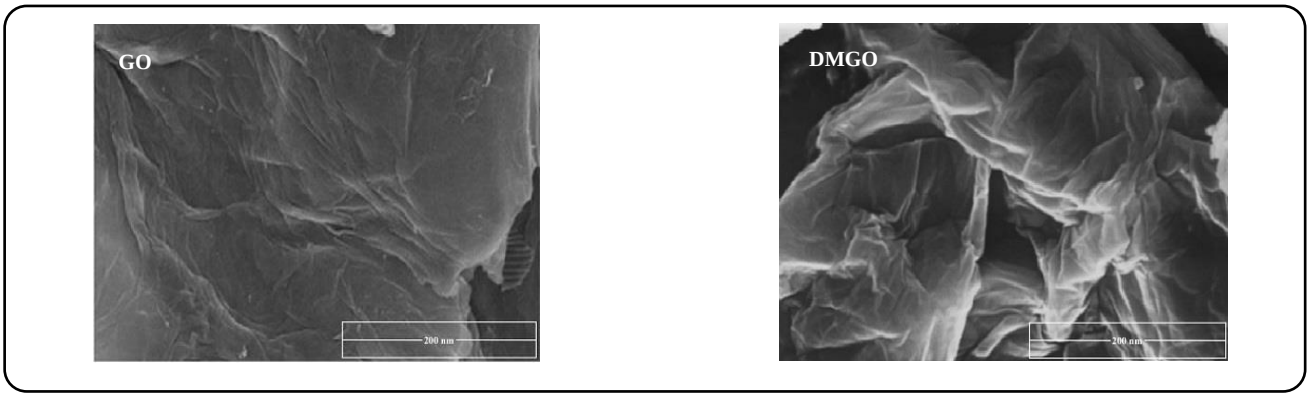

Fig. 3: SEM pattern of MGO and DMGO composite.

the appear of two peaks of 3.4 and 12.5 kev as a result of adsorption of Uranium on the surface of DMGO composite

X-Ray Diffraction (XRD)

The XRD spectrum was used to characterize the GO and DMGO crystalline nature (Fig. 5) the strong diffraction peak of GO is appears at 2θ = 10.7° that correspond to the (001) diffraction with an interlayer distance of approximately 0.82 nm. While the diffraction peak of DMGO move to lower 2θ angle with an interlayer distance 0.98 nm which is larger than GO by 0.16 nm. This increase in the layer to layer distance signifies the impregnation of GO with D2EHPA.

Factor affecting the adsorption of thorium on the surface of DMGO

Effect of pH on adsorption process:

The removal of metal ions from aqueous solution by adsorption is highly depending on the pH of the solution which affects the surface charge of the adsorbent and the degree of ionization and speciation of the adsorbate. Most research has been conducted on heavy metal sorption indicated that the decrease in sorption at acidic pH may be due to the increase in competition with protons for active sites. At the alkaline pH values, however, other effects may arise from some processes, such as the predominant presence of hydrated species of heavy metals, changes in surface charge and the precipitation of the appropriate salt [39, 40]. To verify the effect of pH on U(VI) ions adsorption onto DMGO, experiments were conducted modifying the initial solutions pH from 1 to 5. The obtained results are shown in Fig. 6.

The results show that the pH value is very significant for the performance of DMGO in the process of U(VI) ions adsorption from solution. The adsorption capacity of the DMGO increase sharply at pH range 3–5. At pH > 5 the adsorption capacity decreases with pH increasing. The optimum initial pH of the U(VI) ion solution in the process

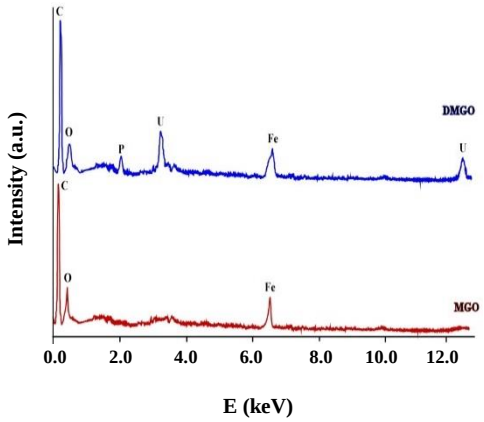

Fig. 4: EDX pattern of MGO and DMGO composite.

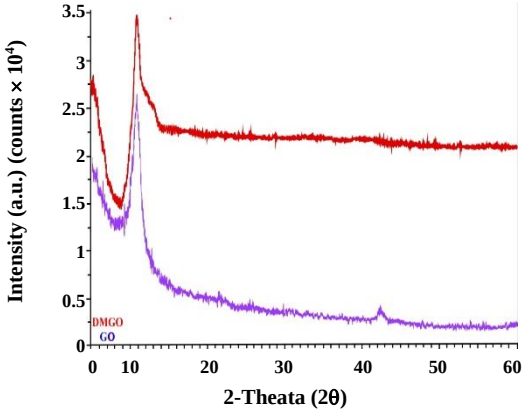

Fig. 5: X-ray diffraction patterns of GO and DMGO.

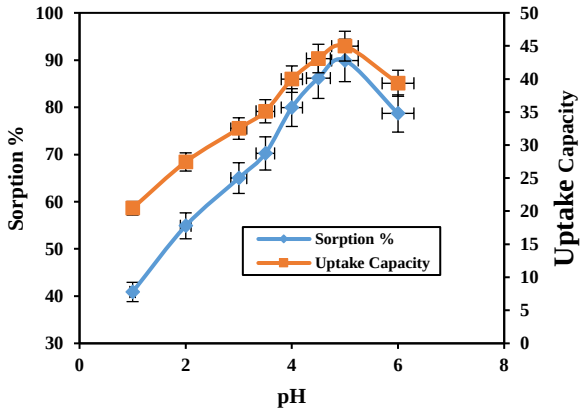

Fig. 6: Effect of equilibrium pH on the extraction of U(VI) with DMGO. U conc. 250 ppm, room temperature, 30 min., contact time, 0.1 gm composite, 20 ml sample).

of U(VI) ions adsorption onto DMGO is 5, where almost 90% of uranium is removed. The further experiments were conducted at an initial pH of the solutions of 5.

Effect of adsorbent dosage on adsorption

The adsorbent amount is an important parameter to obtain the quantitative uptake of metal ion. Fig. 7 shows the adsorption capacity versus weight. The adsorption capacity increase rapidly with increasing the weight of composite from 0.01 until reaching the equilibrium state at 0.1 g. It can be noticed that the adsorption capacity degrease with the resin dosage increasing, therefore this dosage (0.1g) was selected for the all further experimental studies.

Effect of contact time

The effect of contact time on the adsorption of U(VI) studied on the range from 5 to 60 minutes is plotted in Fig. 7. The adsorption efficiency increase gradually with increasing the time reaching the equilibrium at 40 min. and being constant after that, Fig. 8. the short equilibrium time indicates high efficiency and economic feasibility of the sorbent for industrial applications.

In order to investigate the controlling mechanism of adsorption process, the pseudo-first-order and pseudo-second-order kinetic models are used to evaluate the experimental data obtained from batch Th(IV) removal experiments. Pseudo-first-order kinetic model and pseudo second order kinetic model are shown in Eqs. (3) and (4) [41-43].

$$\text{Pseudo-first-order: } \ln(q_e - q_t) = \ln q_e - k_1 t \quad (3)$$

$$\text{pseudo-second-order : } t/q_t = 1/k_2 q_e^2 + 1/q_e\, t \quad (4)$$

Where qe and qt are the amounts of U(VI) adsorbed (mg/g) at equilibrium and at time t (min), respectively. k_1 (min^{-1}) and k_2 (g/mg/min) are the rate constants of pseudo-first order and pseudo-second-order rate constants, respectively.

Kinetic parameters are calculated and shown in Table 1 and (Figs. 9 and 10). Results clearly indicate that the rate of adsorption of U(VI) onto DMGO composite depends on the initial concentration of U(VI). The applicability of these models was quantified from the coefficient of determination, R^2 (Correlation coefficient values). The values of R^2 show that the pseudo-second-order can describe the experimental data better than the pseudo

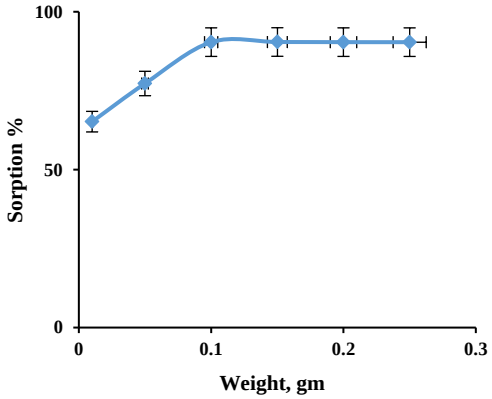

Fig. 7: Effect of adsorbent dosage on the adsorption of U(VI) on DMGO (pH 5, 20ml sample, room temperature, 30 min contact time).

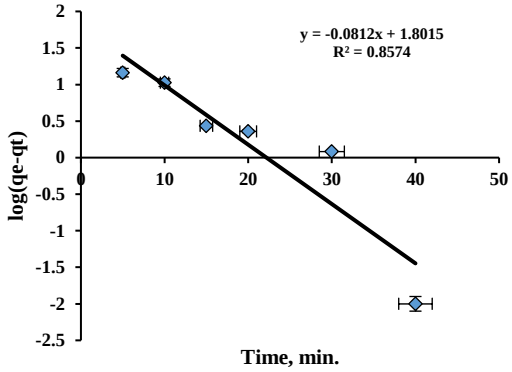

Fig. 9: First order kinetics plot for the adsorption of U (VI) onto DMGO composite.

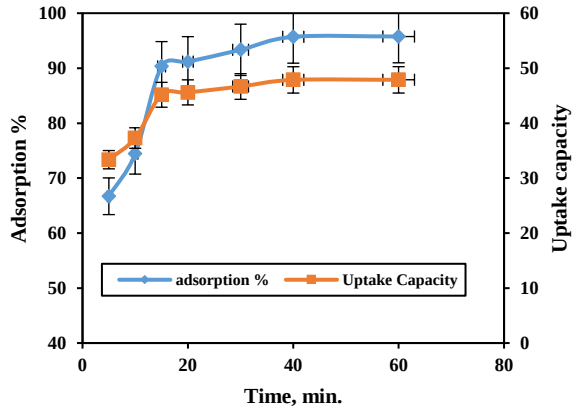

Fig. 8: Effect of contact time on the U(VI) adsorption. (pH 5, 250 ppm U, 20ml sample, room temperature, 0.1 gm. sorbent dosage).

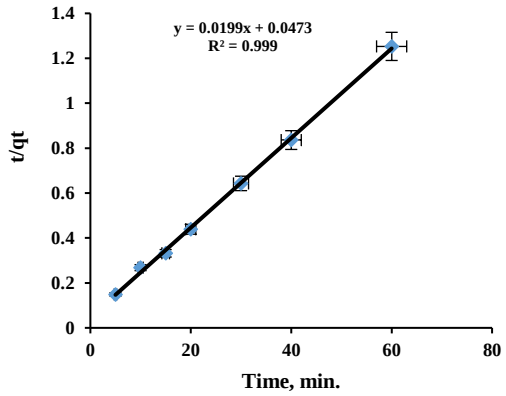

Fig. 10: second order kinetics plot for the adsorption of U (VI) onto DMGO composite.

first-order model. Moreover, the theoretical q_e values calculated from the pseudo second-order model are close to the experimental data. These results confirm the validity of the pseudo second-order model to the adsorption system, suggesting the main adsorption mechanism of chemical adsorption.

Intra-particle diffusion model

In this model, the adsorption of an adsorbate on an adsorbent surface varies proportionately with $t^{0.5}$ according to Weber-Morris equation:

$$q_t = K_{ip} t^{0.5} + I \quad (6)$$

Where K_{ip} is the intra-particle diffusion rate constant and I is a constant proportional to the boundary layer ($mg/g.min^{0.5}$). The larger I value, the greater contribution of the boundary layer [43] .

According to the intra-particle diffusion model, if the value of I is 0, it is means that the intra-particle diffusion is the rate limiting step in the adsorption; if not, the adsorption process is controlled by other adsorption stages, Fig. 11 [45-47]. In this study, intra-particle diffusion is not the main mechanism of the adsorption. As seen from Table 1.

The value of I is 16.68 beside the r^2 is smaller than both 1st and 2nd order kinetics models the pseudo-second-order model could well simulate the data.

Effect of Initial thorium concentration

The effect of initial uranium concentration was studied by using a range of initial thorium concentrations between 50 and 1100 mg/L at three fixed temperatures (298, 323 and 343 K). As shown in Fig.12, the U(VI) uptake capacity increase with the increase in the initial uranium concentration. This may be due to higher metal ion

Table 1:Pseudo-first and second order model parameters of U(VI) sorption onto DMGO.

First ordered Kinetic				2nd ordered Kinetic			Intra-particle diffusion		
K_1	$q_{max(cal)}$	r^2	$q_{max(exp)}$	K_2	$q_{max(cal)}$	r^2	K_{ip}	I	r^2
0.187	63.31	0.999	47.88	0.008	50.25	0.8574	0.7198	16.68	0.839

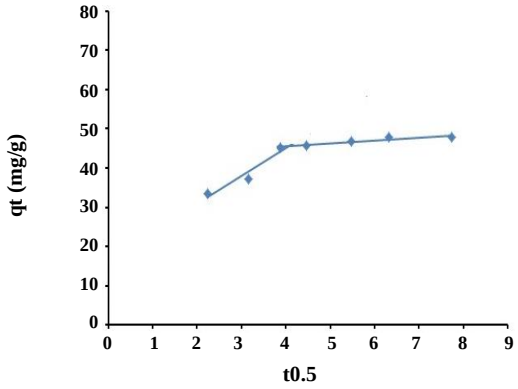

Fig. 11: Intra-particle diffusion model for the adsorption of U (VI) onto DMGO composite.

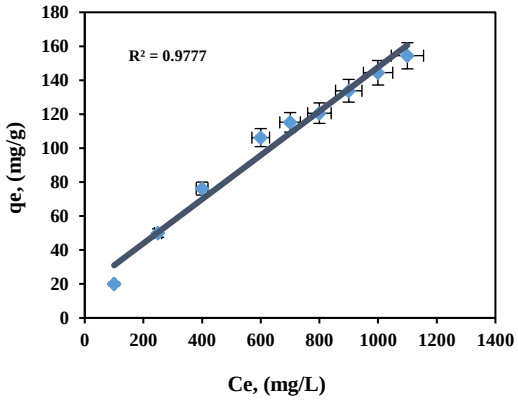

Fig. 12: Effect of initial uranium concentration on U(VI) adsorption efficiency onto DMGO composite.

concentration enhancing the driving force to overcome mass transfer resistance between the aqueous and solid phases [48]. Further, it is observed that the adsorption of uranium by DMGO increase with the increase in temperature indicating that the process to be endothermic in nature.

Sorption isotherms

Adsorption isotherms are very powerful tools for the analysis of adsorption process. Adsorption isotherms establish the relationship between the equilibrium concentration and the amount of adsorbed by the unit mass of adsorbent at a constant temperature. The sorption isotherms of U(VI) ions on DMGO composite are shown in Figs. 13, 14. In order to better understand the sorption mechanism, the experimental data are simulated by the Langmuir and the Freundlich models [49-51]. The Langmuir model assumes that the surface and bulk phases of homogeneous sorbents are of ideal behavior and has been widely used to describe the monolayer sorption process. It is expressed as:

$$\frac{C_e}{q_e} = \frac{1}{b.Q_{max}} + \frac{C_e}{Q_{max}} \qquad (6)$$

Where Q_{max} (in milligrams per gram) represents the maximum amount of metal ions per unit weight of adsorbent to form a complete monolayer on the surface, b is the equilibrium adsorption constant or Langmuir sorption coefficient that represents enthalpy of sorption, q_e is the amount of metal ions adsorbed by adsorbent at equilibrium, and C_e is the equilibrium concentration of Uranium ions.

The linearized Freundlich model is [52, 53]:

$$\ln q_e = \ln k + \left(\frac{1}{n}\right) \ln C_e \qquad (7)$$

Where *1/n* is an indicator of isotherm nonlinearity corresponding to the sorption intensity at a particular temperature and *k* ($mg^{1-n} L^n g^{-1}$) is the Freundlich sorption coefficient related to the sorption capacity of DMGO.

The Langmuir and Freundlich constants evaluated from isotherms and their correlation coefficients of U(VI) sorption on DMGO composite are presented in Table 2.

The Freundlich plot has a correlation coefficient very low; this suggests a restriction on the use of Freundlich isotherms. The numerical value of $1/n < 1$, which provides information about surface heterogeneity and surface affinity for the solute, indicates a very high affinity of the DMGO for U(VI) ions. It is clear that the Langmuir isotherm model provide an excellent fit to the equilibrium adsorption data giving correlation coefficients of 0.9752 and a maximum adsorption capacity close to that determined experimental. The essential feature of

Table 2: Parameters of Langmuir and Freundlich models of U(VI) sorption on DMGO composite.

Langmuir isotherm					Freundlich isotherm		
Temp. ˚C	b	q_m	R^2	q_t	K_f	1/n	R^2
25	0.0255	158.73	0.9752	154.4	38.575	0.2306	0.9317
50	0.0584	169.49	0.9816	166.8	101.555	0.0733	0.6933
70	0.037	181.81	0.9982	179.2	55.322	0.2259	0.9658

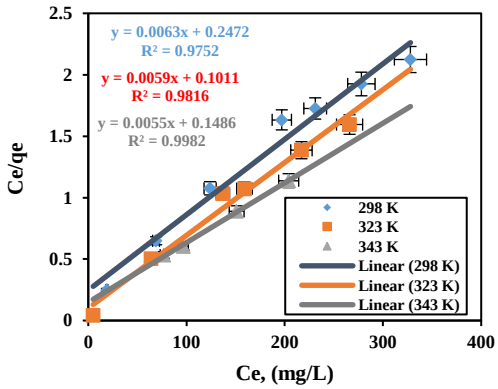

Fig. 13: Langmuir isotherms and of U(VI) ions on DMGO composites.

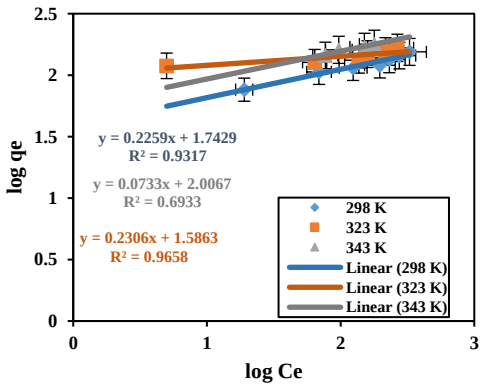

Fig. 14: Freundlich isotherms and of U(VI) ions on DMGO composites.

the Langmuir equation can be expressed in terms of a dimensionless separation factor, R_L defined as:

$$R_L = 1/(1 + K_L C_o) \quad (5)$$

The degree of suitability of the adsorbent towards metal ions was estimated from the values of separation factor constant (RL) (equation 5) which gave indication for the possibility of the adsorption process to be proceed as follow: RL > 1 unsuitable; RL = 1 linear; 0 < RL < 1 suitable; RL = 0 irreversible. The values of RL lie between 0.727 and 0.0425 which indicate the suitability of the adsorbent for U(VI) from aqueous solution.

Also, the observed increase in K_L values with temperature indicates that the adsorption reaction has endothermic nature. This can be confirmed by the calculation of the thermodynamic parameters.

$$\ln K_L = \frac{-\Delta H^{\circ}}{RT} + \frac{\Delta S^{\circ}}{R} \quad (6)$$

$$\Delta G^{o} = \Delta H^{o} - T\Delta S^{o} \quad (7)$$

Thermodynamic parameters (ΔH°, ΔS° and ΔG°) were calculated from the equations listed previously and their values were tabulated in Table 3. The obtained results show that at all studied temperature the values of $|\Delta H^{\circ}| < |T\Delta S^{\circ}|$, The positive value of ΔH° for uranium adsorption indicates that uranium adsorption on DMGO composites is an endothermic process. The positive ΔS°value of uranium also indicates that the adsorption process is spontaneous with high affinity. The negative ΔG° values of uranium also indicate the spontaneous process of uranium sorption under the conditions applied. The decrease of ΔG° with increasing temperature indicates more efficient adsorption at higher temperatures. The thermodynamic parameters reflect the affinity of DMGO composites toward uranium ions in aqueous solutions and may suggest some structural changes in the sorbent [54, 55].

Elution efficiency

The desorption experiments of U(VI) ions are carried out by rinsing the DMGO composites adsorbed U(VI) ions with a series of concentrations (0.01, 0.1, 0.5, 0.75, 1.0 M) of HCl and H_2SO_4 solutions for 5 h under continuous stirring Fig. 15. Then the composite separated by centrifugation and the concentrations of U(VI) in solutions determined with UV Vis spectrophotometer using Arsenazo III as reagent. The experimental results

Table 3: Thermodynamic parameters for adsorption of Th(IV) on composite at different temperatures.

ΔH° (kJ mol^{-1})	ΔS° (J mol^{-1} K^{-1})	ΔG° (kJ mol^{-1})		
5.443	45.25	298 K	323 K	343 K
		-13.48	-14.61	-15.52

Table 4: The Chemical composition of the studied granitic sample.

Major	SiO_2	TiO_2	Al_2O_3	Fe_2O_3*	MnO	MgO	CaO	Na_2O	K_2O	P_2O_5	l.O.I
(%)	73.9	00.54	12.82	02.9	00.04	00.55	00.80	03.35	03.70	00.35	00.95
Trace (ppm)	Ga	U	Rb	Sr	Zr	Ba	Nb	Y	Zn		
	86	755	166	39	244	101	125	107	188		

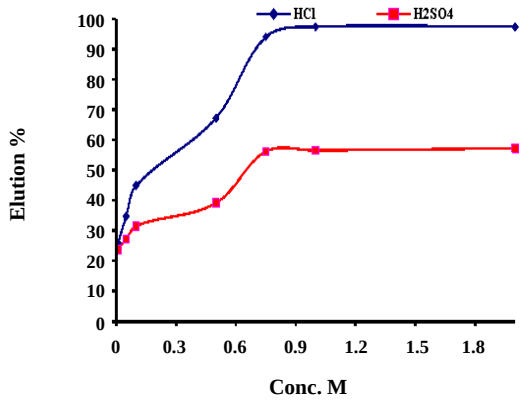

Fig. 13: Langmuir isotherms and of U(VI) ions on DMGO composites.

show that 0.75 M HCl solution is the best eluent giving the best efficiency in comparison with the other concentrations, indicating that DMGO composites have a good desorption property for U(VI) ions under 0.75 M HCl solution, which is suitable for the reusability of the DMGO composite in real possible applications.

The chemical stability of DMGO in acid and alkaline media was tested by shaking a 0.5 g portion of the composite in turn with 100mL of 1M HCl and 1M NaOH for 24h. The composite were then filtered off and washed with water. The adsorption capacities after the treatments were reduced by only 3–5%, which were denoted as desirable stability of the composite. No obvious change of composite was observed in the experimental process. After desorption with 0.75 HCl solution, the residual adsorbed U(VI) ions are negligible, indicating that DMGO composite has a good desorption property for U(VI) ions under 0.75 M HCl solution.

Application on some granitic ore rock samples

This procedure was applied on some rock sample collected from gattar area which is located about 35 km Southwest of Hurghada city, Red Sea coast. The samples of this study are collected from GII uranium prospect which is located in the Northwestern part of Gabal Gattar. Before it's subjected to the chemical analysis, the sample was crushed using the Jaw crusher then ground to about -200 mesh in size by the ball mill. By careful quartering (to conduct complete homogeneity), a 0.5 gram of the ground representative sample was properly digested till complete decomposition and finally obtained in a volume of 250 mL of double distilled water. The major components were identified and estimated by the proper analytical techniques relevant to the measured elements [56], while the trace elements were estimated and the got information were outlined in Table 4. The follow components were evaluated utilizing the nuclear ingestion spectrometer.

0.1 gm of the studied sorbents DMGO was stirring in 20 ml of sample solution at pH 5 for about 40 min. the extraction percentage ($q_{\%}$) was then determined. Table 5, It is was found that adsorption capacity of uranium was about 94.7% by DMGO. Elution of the adsorbed heavy metals was carried out using 0.75M HCl acid.

CONCLUSIONS

Impregnated magnetic graphene oxide in D2EPAH has been prepared, characterized and examined for uranium adsorption from its pregnant solution. The controlling factors have been determined and the obtained results reveal the following: the adsorption of uranium ions onto DMGO is pH dependent with maximum adsorption at pH 5 and reaching the equilibrium after 40 minutes. The experimental maximum adsorption capacities of

Table 5: Effect of DMGO on the uranium concentration of the collected samples.

Gattar Sample	Uranium Concentration (ppm)	Adsorption Efficiency
Adsorption Efficiency	714.99	94.7
Elution Efficiency (0.75M HCl)	697.8	97.6

DMGO is found to be 154.4, 166.8 and 179.2 at 298, 323and 343 K respectively, which indicates that the temperature has a positive effect on uranium adsorption. HCl can be used as desorbing agent for uranium ions from the surface of DMGO.

Conflict of interest

On behalf of all authors, the corresponding author states that there is no conflict of interest.

Received : Feb.. 29, 2019 ; Accepted :Jul. 1, 2019

REFERENCES

[1] D. Brugge, Delemos J.L., Oldmixon B., Exposure Pathways and Health Effects Associated with Chemical and Radiological Toxicity of Natural Uranium: A Review, *Rev. Environ. Health*, **20**: 177-(2005).

[2] Metwally E., Kinetic Studies for Sorption of Some Metal Ions from Aqueous Acid Solutions onto Tda Impregnated Resin, *J. Radional. Nucl. Chem.*, **270**: 559- (2006).

[3] Sharma P., Tomar R., Synthesis and Application of an Analogue of Mesolite for the Removal of Uranium(Vi), Thorium(Iv), and Europium(iii) from Aqueous Waste, *Microporous Mesoporous Mater*, **116**: 641-652 (2008).

[4] Gado M.A., Sorption of Thorium Using Magnetic Graphene Oxide Polypyrrole Composite Synthesized from Natural Source, *Separation Science and Technology*, **53(13)**: 2016-2033 (2018). Doi: 10.1080/01496395.2018.

[5] Cecal A., Humelnicu D., Rudic V., Cepoi L., Ganju D., Cojocari A., Uptake of Uranyl Ions from Uranium Ores and Sludges by Means of Spirulina Platensis, Porphyridium Cruentum and Nostok Linckia Alga, *Bioresour Technol*, **118**:19–23 (2012).

[6] Hierro A., Martın Je., Olıas M., Vaca F., Bolivar Jp., Uranium Behaviour in an Estuary Polluted by Mining and Industrial Effluents: the Rıa of Huelva (Sw of Spain), *Water Res.*, **47**:6269–6279 (2013).

[7] Tan Lc., Wang J., Liu Q., Sun Yb., Zhang Hs., Wang Yl., Jing Xy., Liu Jy., Song Dl., Facile Preparation of Oxine Functionalized Magnetic Fe_3O_4 Particles for Enhanced Uranium(Vi) Adsorption, *Colloid Surf A*, **466**:85–91 (2015).

[8] Zhang Cd., Dodge Cj., Malhotra Sv., Francis Aj., Bioreduction and Precipitation of Uranium Inionic Liquid Aqueous Solution by Clostridium Sp., *Bioresour Technol.*, **136**:752–756 (2013).

[9] Tapia-Rodriguez A., Luna-Velasco A., Field Ja., Sierra-Alvarez R., Anaerobic Bioremediation of Hexavalent Uranium in Groundwater by Reductive Precipitation with Methanogenic Granular Sludge, *Water Res.*, **44**: 2153–2162 (2010).

[10] Shen Jj., Schafer A., Removal of Fluoride and Uranium by Nanofiltration and Reverse Osmosis: A Review, *Chemosphere*, **117**: 679–691 (2014).

[11] Sreenivas T., Rajan Kc., Studies on the Separation of Dissolved Uranium from Alkaline Carbonate Leach Slurries by Resin-In- Pulp Process, *Sep Purif Technol*, **112**: 54–60 (2013).

[12] Li J., Zhang Y., Remediation Technology for the Uranium Contaminated Environment: A Review, *Procedia Environ Sci.*, **13**:1609–1615 (2012).

[13] Yu J., Bai H., Wang J., Li Z., Jiao C., Liu Q., Zhang M., Liu L., Synthesis of Alumina Nanosheets *via* Supercritical Fluid Technology with High Uranyl Adsorptive Capacity, *New. J. Chem.*, **37**: 366–372 (2013).

[14] Bai Z.Q., Yuan l.-Y., Zhu L., Liu Z.-R., Chu Sh.-Q., Zheng L.-R., Zhang J., Chai Z.-F., Shi W.-Q., Introduction of Amino Groups Into Acid-Resistant Mofs for Enhanced U(Vi) Sorption, *J. Mater. Chem. A*, **3**: 525-534 (2014).

[15] Barber P.S., Griggs C.S., Rogers R.D., Kelley S.P., Wallace S., Surface Modification of Ionic Liquid-Spun Chitin Fibers for the Extraction of Uranium from Seawater: Seeking the Strength of Chitin and the Chemical Functionality of Chitosan, *Green Chem.*, **4**: 1828–1836 (2014).

[16] Roberto J.B., Rubia T.D., Basic Research Needs for Advanced Nuclear Energy Systems, *Jom*, **59**: 16–19 (2007).

[17] Du J., Lai X., Yang N., Zhai J., Kisailus D., Su F., Wang D., Jiang L., Hierarchically Ordered Macro−Mesoporous TiO2− Graphene Composite Films: Improved Mass Transfer, Reduced Charge Recombination, and Their Enhanced Photocatalytic Activities, *ACS Nano*, **5**: 590–596 (2010).

[18] Negm S.H., Abd El-Hamid A.A.M., Gado M.A., El-Gendy H.S., Selective Uranium Adsorption Using Modified Acrylamide Resins, *Journal of Radioanalytical and Nuclear Chemistry* (2018). Doi:10.1007/S10967-018-6356-5

[19] Fang J., Gao B., Mosa A., Zhan L., Chemical Activation of Hickory and Peanut Hull Hydrochars for Removal of Lead and Methylene Blue from Aqueous Solutions, *Chem. Speciat. Bioavailab.*, **29**: 197–204 (2017).

[20] Fang J., Zhan L., Ok Y.S., Gao B., Minireview of Potential Applications of Hydrochar Derived from Hydrothermal Carbonization of Biomass, *J. Ind. Eng. Chem.*, **57**: 15–21 (2018).

[21] Inyang M., Gao B., Zimmerman A., Zhang M., Chen H., Synthesis, Characterization, and Dye Sorption Ability of Carbon Nanotube–Biochar Nanocomposites, *Chem. Eng. J.*, **236**: 39–46(2014).

[22] Gado M.A., Khattab M.R., Atia B.M., Modification of Uranium Determination Procedures by Alpha Spectrometry Using Graphene Oxide Functionalized 4-Aminobenzenesulfonate, *Sn Applied Sciences*, 1**(5)** (2019). Doi:10.1007/S42452-019-0462-Z

[23] Chen H., Gao B., Li H., Removal of Sulfamethoxazole and Ciprofloxacin from Aqueous Solutions by Graphene Oxide, *J. Hazard. Mater.*, **282**: 201–207 (2015).

[24] Gu D., Fein J.B., Adsorption of Metals Onto Graphene Oxide: Surface Complexation Modeling and Linear Free Energy Relationships, *Colloids Surf. A Physicochem. Eng. Asp.*, **481**: 319–327 (2015).

[25] Paredes J., Villar-Rodil S., Martinez-Alonso A., Tascon J., Graphene Oxide Dispersions in Organic Solvents, *Langmuir*, **24**: 10560–10564 (2008).

[26] Madadrang C.J., Kim H.Y., Gao G., Wang N., Zhu J., Feng H., Hou S., Adsorption Behavior of Edta-Graphene Oxide for Pb (Ii) Removal, *Acs Applied Materials & Interfaces*, **4(3)**: 1186–1193 (2012). Doi:10.1021/Am201645g

[27] Peng W., Li H., Liu Y., Song S., A Review on Heavy Metal Ions Adsorption from Water by Graphene Oxide and Its Composites, *Journal of Molecular Liquids*, **230**: 496–504 (2017). Doi:10.1016/J.Molliq.2017.01.064

[28] Sitko R., Turek E., Zawisza B., Malicka E., Talik E., Heimann J., Gagor A., Feist B., Wrzalik R., Adsorption of Divalent Metal Ions from Aqueous Solutions Using Graphene Oxide, *Dalton Transactions*, **42(16)**: 5682- (2013). Doi:10.1039/C3dt33097d

[29] Wang Z., Zhu W., Qiu Y., Et Al. Biological and Environmental Interactions of Emerging Two-Dimensional Nanomaterials, *Chem Soc Rev.*, **45**: 1750–1780 (2016).

[30] Shao D., Hou G., Li J., Wen T., Ren X., Wang X., Pani/Go as a Super Adsorbent for the Selective Adsorption of Uranium(Vi), *Chemical Engineering Journal*, **255**: 604–612 (2014). Doi:10.1016/J.Cej.2014.06.063

[31] Liu S., Ouyang J., Luo J., Sun L., Huang G., Ma J., Removal of Uranium(Vi) from Aqueous Solution Using Graphene Oxide Functionalized with Diethylenetriaminepentaacetic Phenylenediamine. *Journal of Nuclear Science and Technology*, **55(7)**: 781–791 (2018). Doi:10.1080/00223131.2018.1439415

[32] Kim J., Cote L.J., Kim F., Yuan W., Shull K.R., Huang J., Graphene Oxide Sheets at Interfaces, *Journal of American Chemical Society*, 9, 132: 818 (2010).

[33] Chenlu B., Lei S., Weiyi X., Bihe Y., Charles A.W., Jianliu H., Yuqiang G., Yuan H., Preparation of Graphene by Pressurized Oxidation and Multiplex Reduction and its Polymer Nanocomposites by Masterbatch- Based Melt Blending, *Journal of Materials Chemistry*, **22**: 6088- (2012).

[34] Massart R., Preparation of Aqueous Magnetic Liquids in Alkaline and Acidic Media, *Ieee Transactions Magnetic*, **17**: 1247- (1981).

[35] Goods J.B., Sydlik S.A., Walish J.J., Swager T.M., Phosphate Functionalized Graphene with Tunable Mechanical Properties, *Advanced Materials*, **26(5)**: 718–723 (2013). Doi:10.1002/Adma.201303477

[36] Liu X., Li J., Wang X., Chen C., Wang X., High Performance of Phosphate-Functionalized Graphene Oxide for the Selective Adsorption of U(Vi) from Acidic Solution, *Journal of Nuclear Materials*, **466**: 56–64 (2015).
Doi:10.1016/J.Jnucmat.2015.07.027

[37] Zhao G., Li J., Ren X., Chen C., Wang X., Few-Layered Graphene Oxide Nanosheets as Superior Sorbents for Heavy Metal Ion Pollution Management, *Environmental Science & Technology*, **45(24)**: 10454–10462 (2011).
Doi:10.1021/Es203439v

[38] Gado M.A., Morsy A., Preparation of Poly-Aniline-Magnetic Porous Carbon Composite for Using as Uranium Adsorbent, *American J. Materials Synthesis and Processing*, **3**: 32- (2017).

[39] Afifi S., Mustafa M., El Sheikh E., Gado M.A.S., Extraction and Determination of Thorium and Its Application on Geologic Samples Using Trioctyl Phosphine Oxide, *Arab. J. Nucl. Sci. Appl.*, **45(3)**: 1–16 (2012).

[40] Kula I., Ugurlu M., Karaoglu H., Celik A., Adsorption of Cd(Ii) Ions from Aqueous Solutions Using Activated Carbon Prepared from Olive Stone by $ZnCl_2$ Activation, *Bioresour. Technol.*, **99**: 492–501 (2008).

[41] Manju G.N., Raji C., Anirudhan T.S., Evaluation of Coconut Husk Carbon for the Removal of Arsenic from Water, *Water Res.*, **32**: 3062–3070 (1998).

[42] Gado M.A., Atia B.M., Adsorption of Thorium Ions Using Trioctylphosphine Oxide Impregnated Dowex 1×4 Powder, *Radiochemistry*, **61(2)**: 168–176 (2019).
Doi:10.1134/S1066362219020061

[43] Ho Y.S, Mckay G., Pseudo-Second Order Model for Sorption Processes, *Process. Biochem.*, **34**: 451-465 (1999).

[44] Ojedokun A.T., Bello O.S., Kinetic Modeling of Liquid-Phase Adsorption of Congo Red Dye Using Guava Leaf-Based Activated Carbon, *Appl. Water Sci.* (2016).
Doi 10.1007/S13201-015-0375-Y.

[45] Li Y., Yue Q., Gao B., Adsorption Kinetics and Desorption of Cu(Ii) and Zn(Ii) from Aqueous Solution onto Humic Acid, *Journal of Hazardous Materials*, **178 (1–3)**: 455–461 (2010).
Doi:10.1016/J.Jhazmat.2010.01.103.

[46] Zhang Y., Li Y., Ning Y., Liu D., Tang P., Yang Z., Wang X., Adsorption and Desorption of Uranium(Vi) onto Humic Acids Derived From Uranium-Enriched Lignites, *Water Science and Technology*, **77(4)**: 920–930 (2017).
Doi:10.2166/Wst.2017.608

[47] Atia B.M., Gado M.A., Cheira M.F., Kinetics of Uranium and Iron Dissolution by Sulfuric Acid from Abu Zeneima Ferruginous Siltstone, Southwestern Sinai, Egypt, *Euro-Mediterranean Journal for Environmental Integration*, **3(1)**: - (2018).
Doi:10.1007/S41207-018-0080-Y

[48] Wang H.L., Hao Q.L., Yang X.J., Lu L.D., Wang X., Graphene Oxide Doped Polyaniline for Supercapacitors, *Electrochem Communicable*, **11**: 1158-1161 (2009).

[49] Langmuir, The Constitution and Fundamental Properties of Solids and Liquids, *J. Am. Chem. Soc.*, **38**: 2221–2295 (1916).

[50] Ma G., Aa A., Sa Z., Synthesis of Amino Magnetic Titano-Silicate and Its Role for Uranium Adsorption, *Advances in Recycling & Waste Management*, **02**(03): 2-4 (2017).
Doi:10.4172/2475-7675.1000147

[51] Gado M.A., Morsy A., Preparation of Poly-Aniline–Magnetic Porous Carbon Composite for Using as Uranium Adsorbent, *Am. J. Mater. Synth. Process*, **2**: 32–40 (2017)

[52] Freundlich M.F., Uber Die Adsorption in Lasungen, *Z. Phys. Chem.*, **57**: 385–470 (1906).

[53] Amer T.E., El-Sheikh E.M., Gado M.A., Abu-Khoziem H.A., Zaki S.A., Selective Recovery of Lanthanides, Uranium and Thorium From Rosetta Monazite Mineral Concentrate, *Separation Science and Technology*, **53(10)**: 1522–1530 (2017).
Doi:10.1080/01496395.2017.1405039

[54] Genc-Fuhrman H., Tjell J., Mcconchie D., Adsorption of Arsenic from Water Using Activated Neutralized Red Mud, *Environ. Sci. Technol.*, **38**: 2428 (2004).

[55] Wang X., Lu J., Xing B., Sorption of Organic Contaminants by Carbon Nanotubes: Influence of Adsorbed Organic Matter, *Environ. Sci. Technol.*, **42**: 3207 (2008).

[56] Shapiro L., Rapid Analysis of Silicate, Carbonate and Phosphate Rocks, *U. S. Geol. Surv.Bull.*, **1401**: 70-76 (1975).